Brain Structure and Function (2023) 228:121–130
https://doi.org/10.1007/s00429-022-02555-1

ORIGINAL ARTICLE

The connectivity-based parcellation of the angular gyrus: fiber dissection and MR tractography study

Fatih Yakar[1] · Pınar Çeltikçi[2] · Yücel Doğruel[3] · Emrah Egemen[1] · Abuzer Güngör[3,4]

Received: 5 January 2022 / Accepted: 14 August 2022 / Published online: 3 September 2022

Abstract

The angular gyrus (AG) wraps the posterior end of the superior temporal sulcus (STS), so it is considered a continuation of the superior temporal gyrus (STG)/ middle temporal gyrus (MTG) and forms the inferior parietal lobule (IPL) with the supramarginal gyrus (SMG). The AG was functionally divided in the literature, but there is no fiber dissection study in this context. This study divided AG into superior (sAG) and inferior (iAG) parts by focusing on STS. Red, blue silicone-injected eight and four non-silicone-injected human cadaveric cerebrums were dissected via the Klingler method focusing on the AG. White matter (WM) tracts identified during dissection were then reconstructed on the Human Connectome Project 1065 individual template for validation. According to this study, superior longitudinal fasciculus (SLF) II and middle longitudinal fasciculus (MdLF) are associated with sAG; the anterior commissure (AC), optic radiation (OR) with iAG; the arcuate fasciculus (AF), inferior frontooccipital fasciculus (IFOF), and tapetum (Tp) with both parts. In cortical parcellation of AG based on STS, sAG and iAG were associated with different fiber tracts. Although it has been shown in previous studies that there are functionally different subunits with AG parcellation, here, for the first time, other functions of the subunits have been revealed with cadaveric dissection and tractography images.

Keywords Angular gyrus · Superior temporal gyrus · Inferior temporal gyrus · Tractography · Fiber dissection · White matter

Introduction

The angular gyrus (AG) has extensive white matter (WM) connections with sensory and motor association cortices and classic language areas like the inferior frontal and superior temporal regions (Price et al. 2015). It involves the semantic process, reading and comprehension, the default network, number processing, attention and spatial/social cognition, and reasoning (Seghier 2013). It also shows robust activation across a range of tasks proposed to engage the episodic memory system, simulating possible events in the future and remembering events from the past (Ramanan et al. 2018). The AG is located at the junction of the temporal, parietal, and occipital lobes (Seghier 2013). It can be identified with its horseshoe shape near the dorsal-posterior segment of the superior temporal sulcus (STS) (Naidich et al. 1995). It wraps the posterior end of the STS (Rhoton 2007) and forms the inferior parietal lobule (IPL) with the supramarginal gyrus (SMG) (Binder et al. 2009). It is a posterior component of the IPL (Kiriyama et al. 2009). These two gyri are located vertically at the hemisphere surface, and the U fibers connecting them are horizontally located (Sarubbo et al. 2016). The AG was functionally divided by different authors (Seghier et al. 2010; Wang et al. 2012, 2017; Seghier 2013); however, there is no fiber dissection study in this context. This study aims to examine possible functional

✉ Abuzer Güngör
abuzergungor@gmail.com

1 Department of Neurosurgery, Pamukkale University School of Medicine, Çamlaraltı, Kınıklı Cd No. 37, 20160 Pamukkale/Denizli, Turkey

2 Department of Radiology, Ankara City Hospital, Üniversiteler Mahallesi 1604. Cadde No. 9, 06800 Çankaya/Ankara, Turkey

3 Department of Neurosurgery, Yeditepe University School of Medicine, İçerenköy Mahallesi Hastane Sokak No. 4 D:4/1, 34854 Istanbul, Turkey

4 Department of Neurosurgery, Bakirköy Research and Training Hospital for Psychiatry, Neurology, and Neurosurgery, Zuhuratbaba Mah, Dr. Tevfik Sağlam Cd No. 11, 34147 Bakırköy/Istanbul, Turkey

differences based on WM connectivity between the superior and inferior parts of the angular gyrus.

Methods

All abbreviations in the study are provided in Table 1.

Preparation of specimens and fiber dissection

Red, blue silicone-injected eight human cadaveric cerebrums and four non-silicone-injected cerebrums (pia, arachnoid, and vascular structures were removed), fixed in 5% formalin for 2 months and then frozen at −10 °C for 15 days, were defrosted and preserved at room temperature. The formalin solution generally does not penetrate the myelinated fibers and the volume of water that turns into the ice after freezing increases by 10%. Thus, it causes the fibers to separate from each other, and dissection can be performed easily. Lateral hemispheric dissection was performed with the Klingler method (Dziedzic et al. 2021), focusing on superior and inferior parietal lobule. Metal and wooden spatulas were used during dissection, and the hemispheres were preserved with wet swabs. All fiber tracts adjacent to the AG were dissected, and synchronous MR tractography images were given stepwise.

To be able to orient the surface anatomy and the AG, the following anatomical structures were identified in the first step: central sulcus, pre/postcentral gyrus, postcentral sulcus, intraparietal sulcus, lateral sulcus, and STS. The area behind the postcentral sulcus is divided by the intraparietal sulcus into the superior parietal lobule (SPL) and IPL. The IPL consists of the SMG and AG (Cikla et al. 2016). The structures that wrap the posterior end of the lateral sulcus and the STS are described as SMG and AG, respectively (Rhoton 2007). The AG is limited by descending portion of the sulcus intermedius anteriorly (Ribas 2010) and by the dorsal part of the anterior occipital sulcus posteriorly (Rademacher et al. 1992). These sulci demarcate the AG from SMG and occipital lobe, respectively (Fig. 1a, b). The dissection was performed on the lateral surface of the hemisphere.

Table 1 All abbreviations in the study according to the order in the text

Abbreviation	Explanation
MRI	Magnetic resonance imagination
AG	Angular gyrus
STS	Superior temporal sulcus
STG	Superior temporal gyrus
MTG	Middle temporal gyrus
IPL	Inferior parietal lobule
SMG	Supramarginal gyrus
sAG	Superior angular gyrus
iAG	Inferior angular gyrus
WM	White matter
SLF	Superior longitudinal fasciculus
MdLF	Middle longitudinal fasciculus
Th	Thalamus
AC	Anterior commissure
OR	Optic radiation
AF	Arcuate fasciculus
IFOF	Inferior frontooccipital fasciculus
Tp	Tapetum
SPL	Superior parietal lobule
IFG	Inferior frontal gyrus
MFG	Middle frontal gyrus
SS	Sagittal stratum
CR	Corona radiata
ExC	Extreme capsule
UF	Uncinate fasciculus
EC	External capsule
IC	Internal capsule

Division of the AG

The AG is divided into two parts by their position to STS in this study. The upper front part was named superior angular gyrus (sAG), and the lower back part was named inferior angular gyrus (iAG). The analyses of the dissections were focused on the differences between the sAG and iAG. AG-related fiber tracts were classified as associated with sAG, iAG, or both (Table 2).

Fiber tracking

To confirm fiber dissection findings, tracts of interest were reconstructed using tractography. All fiber tracking was performed with DSI-Studio (http://dsi-studio.labsolver.org) on a group average template constructed from a total of 1065 subjects from the Human Connectome Project (publicly available at http://dsi-studio.labsolver.org). A deterministic fiber tracking algorithm was used with a multishell diffusion scheme, and the *b*-values were 990, 1985, and 2980 s/mm^2. The number of diffusion sampling directions was 90, 90, and 90, respectively. The in-plane resolution was 1.25 mm, and the slice thickness was 1.25 mm. The diffusion data were reconstructed in the Montreal Neurological Institute space using q-space diffeomorphic reconstruction to obtain the spin distribution function (Yeh and Tseng 2011). Fiber tracking was initiated following selected regions of interest placement on the quantitative anisotropy map until 100.000 streamlines were detected. Fiber progression continued with an anisotropy threshold of 0.156, the angular threshold of

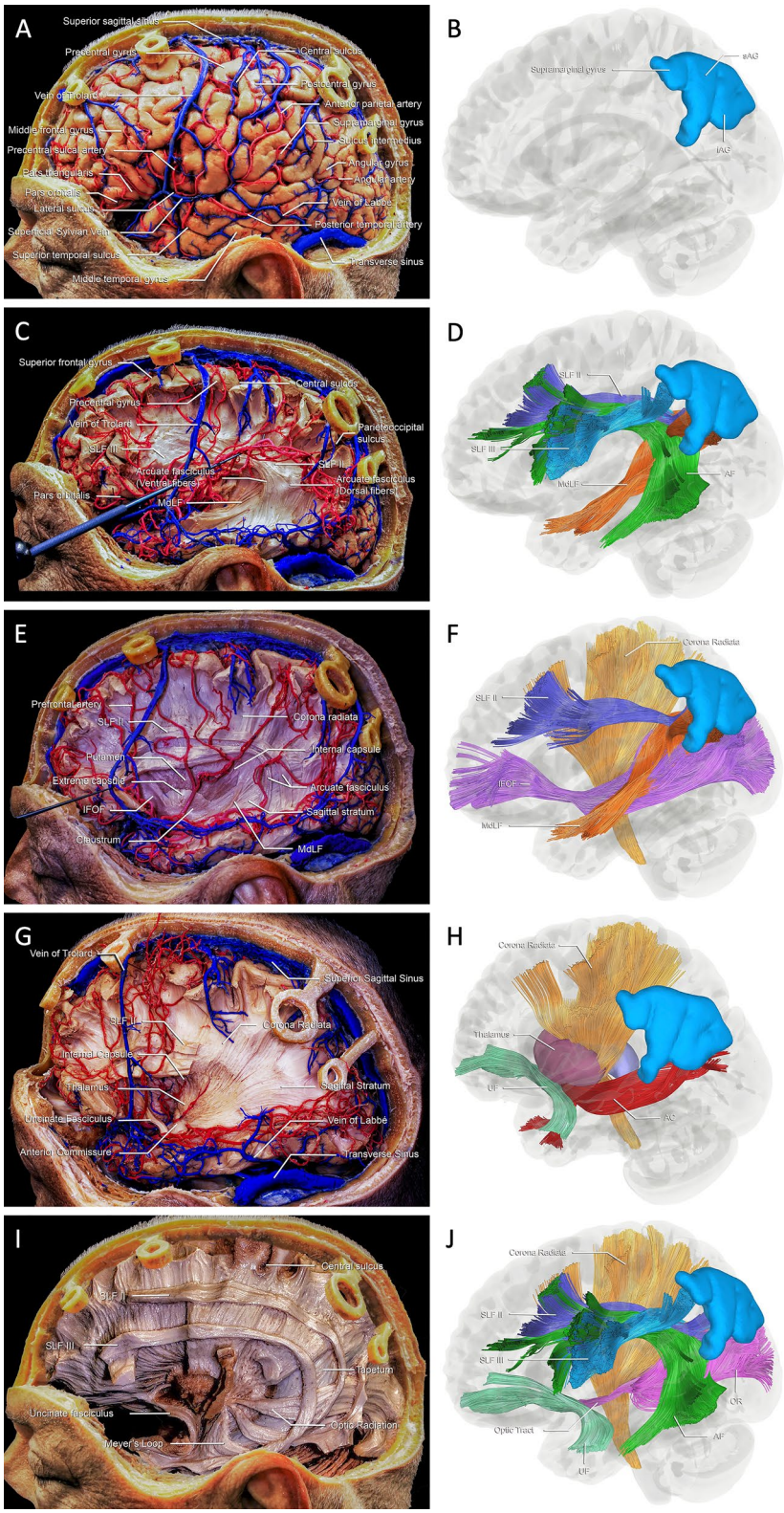

Fig.1 Fiber dissection and tractography images demonstrate fiber pathways associated with the angular gyrus. **a** Superficial cortical and vascular anatomy on a red–blue silicone-injected cadaveric head. **b** The projection of the angular gyrus is demonstrated on the MR tractography image. **c** MdLF and SLF II pass through sAG, AF pass through both sAG and iAG. **d** The pathways shown in 1c are presented on the tractography. **e** IFOF fibers pass through both the sAG and the iAG. **f** The course of IFOF fibers and their relationship with MdLF and SLF II is presented on tractography. **g** AC fibers do not pass through the sAG while passing through the iAG in the occipital projection. **h** The relation of AC fibers with iAG is shown in the tractography image. **i** A non-silicone-injected hemisphere is presented within the cadaveric skull in the previous figures to preserve anatomical orientation. **j** OR fibers pass through the iAG only, and tapetum fibers pass through both angular gyrus segments. *sAG* superior angular gyrus, *iAG* inferior angular gyrus, *SLF* superior longitudinal fasciculus, *MdLF* middle longitudinal fasciculus, *AF* arcuate fasciculus, *IFOF* inferior frontooccipital fasciculus, *UF* uncinate fasciculus, *AC* anterior commissure, *OR* optic radiation

45–60 depending on the fiber tract, and step size was randomly selected from 0.5 to 1.5 voxels. Tracks with a length shorter than 30 or longer than 300 mm were discarded. False or overlapping tracts that did not correspond to the known anatomical limits of the tract of interest were manually deleted. Fiber tracts were validated by qualitative comparison with the conventional magnetic resonance images over which reconstructed tracts were displayed and fiber

Table 2 Fiber tracts related to sAG, iAG, or both

Fibers	sAG	iAG	Both
SLF II	+		
AF			+
MdLF	+		
IFOF			+
AC		+	
OR		+	
Tp			+

sAG superior angular gyrus; *iAG* inferior angular gyrus; *SLF II* superior longitudinal fasciculus II; *AF* arcuate fasciculus; *MdLF* middle longitudinal fasciculus; *IFOF* inferior frontooccipital fasciculus; *AC* anterior commissure; *OR* optic radiation; *Tp* tapetum

dissection images. Final tractography images were displayed over a three-dimensional surface image of the brain using the 'Surface Rendering' tool on the software. Fiber tracking and validation were performed by a neuroradiologist with 5 years of fiber tracking analysis experience.

Results

The cortical gray matter of the inferior frontal gyrus (IFG)/middle frontal gyrus (MFG), the inferior part of the pre/postcentral gyrus, the SMG/AG, and the superior temporal gyrus (STG)/middle temporal gyrus (MTG) and U fibers were removed. Superior longitudinal fasciculus (SLF) II/III, arcuate fasciculus (AF), and middle longitudinal fasciculus (MdLF) were revealed. SLF III lies inferior and lateral to SLF II, and there is no clear demarcation between these structures. The connections between the AG-MFG/IFG and the SMG-IFG are provided by SLF II and III, respectively. AF wraps around the posterior edge of the insula like a horseshoe and establishes the connection between the middle/superior temporal gyri and inferior/middle frontal gyri. The MdLF connects the temporal pole and STG to the angular gyrus and superior occipital lobe. Our dissections indicate that the SLF II lies between the MFG and sAG and has no connections with the iAG. On the other hand, the SLF III starts from IFG, terminates at SMG, and does not give fiber branches to AG. However, the dorsal part of the AF creates a similar shape to the AG and has connections with both sAG and iAG (Fig. 1c, d).

Dissection of the temporal lobes gray matter and U fibers exposed the MdLF fibers. The MdLF projects a straight route from the temporal pole to the superior parietal lobule above the STS. Therefore, MdLF fibers have connections with sAG and not iAG. After the MdLF fibers emerge from the STG, they merge with the sagittal stratum (SS) fibers. SS fibers are located medial to the AF/SLF complex and lateral to the tapetal fibers of the atrium (Di Carlo et al. 2019). Corona Radiata (CR) and SS were revealed when the dissection was deepened on the lateral aspect of the hemisphere, keeping the SLF II and AF as a strip. Removing the insular gray matter exposed the extreme capsule (ExC). After removing ExC, the claustrum at the apex of the insula and the inferior frontooccipital fasciculus (IFOF) were revealed in the limen insula (Fig. 1e, f).

The IFOF courses medial to the MdLF, starting from the inferior and middle frontal gyri and extending through the temporal, occipital lobes, and the superior parietal lobule (Martino et al. 2010). According to the dissections and tractography analyses, IFOF reaches both sAG and iAG. When the superficial dorsal fibers of IFOF pass through the sAG, the deep ventral fibers pass through the iAG. The vascular structures retracted to present the IFOF and MdLF more clearly. After removing IFOF, the uncinate fasciculus (UF) was exposed (Fig. 1g, h). The UF passes just under the IFOF and connects orbitofrontal/septal areas to the anterior part of the temporal lobe. The IFOF and UF form the ventral portion of the external capsule (EC) (Ribas et al. 2018).

The strip of SLF II and AF was removed, and the internal capsule (IC) fibers were exposed at a depth of dissection along the CR. The CR fibers (fan-shaped, projection fibers between the cerebral cortex, brainstem, and spinal cord) were inferiorly converged as IC. Deep temporal dissection revealed the anterior commissure (AC) fibers and the thalamus (Th). The AC consists of a body and anterior/posterior parts. The body of AC crosses the midline at the anterior wall of the third ventricle and divides into anterior/posterior parts. The posterior part gives extensions to temporal and occipital lobes. The occipital extension of the AC travels lateral to the temporal horn and atrium. Our analyses support that the AC fibers travel through the iAG below the sAG (Fig. 1g, h). Removing the AC fibers exposes the optic radiation. It has been reported that optic radiation consists of three subgroups of fibers. The anterior fibers of the optic radiation (OR) pass through the lateral aspect of the temporal horn and the floor of the atrium. In addition, our dissection demonstrates a relationship between the iAG and the OR by following these fibers in the posterior route. The last stage of our dissection reveals tapetum (Tp) fibers between the OR and the lateral ventricle (Pastor-Escartín et al. 2019). Tp fibers surround the lateral wall and the roof of the atrium, occipital and temporal horns of the lateral ventricles. Our observations show the Tp fibers run deep in sAG and iAG (Fig. 1i, j).

SLF II, III, IC, UF, and Th were preserved in a different hemisphere until the last stage. The OR and Meyer loop

were revealed when the SS and AC fibers were removed. In addition, the roof, lateral wall, and one-third of the lateral part of the floor of the temporal horn were covered by OR fibers. Finally, by removing the CR fibers, the Tp structure surrounding the atrium, occipital and temporal horn of the lateral ventricle was revealed (Fig. 1i, j). In addition, a separate hemisphere dissection without vascular structures is given in Fig. 2, considering that the vascular structures may prevent the clear visualization of normal anatomical structures.

Discussion

The WM anatomy of the temporal, parietal, and occipital lobe (Kiriyama et al. 2009; Burks et al. 2017; Kadri et al. 2017; Ripollés et al. 2017; Saalasti et al. 2019; Jitsuishi and Yamaguchi 2020; Briggs et al. 2021; Egemen et al. 2021) and junction (Biceroglu and Karadag 2019) has been extensively studied in the literature. Previously, Yagmurlu et al. (2015) divided AG into upper and lower parts by evaluating only the SLF II and AF. In our study, the AG was divided into two parts (superior and inferior), and the WM fibers associated with its parts were compared. Consequently, SLF II and MdLF are associated with sAG; the AC, OR with iAG; the AF, IFOF, and Tp with both parts. To the best of our knowledge, this is the first anatomical study dividing the AG into two parts to evaluate all fiber tracts according to these parts. According to our study, in sAG or iAG injury, transcortical motor aphasia, phonological paraphasia, repetition disorder aphasia (AF injury), semantic paraphasias, orthography-phonology translation (nonword reading) (IFOF injury), and contralateral epileptiform activities, auditory or visual disconnection syndromes (Tp injury) occur. However, Gerstmann syndrome and spatial hemineglect (SLF II injury) will be observed in the isolated damage of the sAG, while verbal anosmia, quadrantanopia, and macular visual defects will occur in the isolated damage of the iAG (Table 3).

A functional MRI study (Seghier et al. 2010) divided left AG into three parts: mid, dorsomedial, and ventrolateral regions. It has been stated that regardless of the presence of the stimulus, the mid-region is involved in semantic associations, the dorsomedial region is in search of semantics in all visual stimulations, and the ventrolateral region is in the conceptual identification of visual inputs. According to the anatomical classification in our study, approximately the dorsomedial region corresponds to sAG and the ventrolateral and mid-region to iAG. A tractography-based parcellation study divided IPL into five clusters (Mars et al. 2011). The activity was recorded when people redirected visuospatial attention from one location to another in tractography corresponding to the anterior part of AG and when people successfully retrieved memories in the posterior part of AG. The classification in this study was not correlated with the classification in our study. In another study (Wang et al. 2017), AG was parcelled as dorsal and ventral parts. The dorsal part had associations with the frontal pole, superior frontal gyrus, MFG, pre-supplementary motor area, middle MTG, and dorsal lateral prefrontal cortex (DLPFC). The ventral part had associations with DLPFC, anterior MTG, precuneus, medial prefrontal cortex, anterior and posterior parahippocampus. In the tractography-based study conducted by Wang et al. (2012), IPL was divided into five clusters, but the cluster containing AG also included the ventral premotor cortex and IFG. In a recent study (Sarubbo et al. 2020), human neural functions, cortical and subcortical structures were evaluated by real-time neurophysiological testing. This study observed the functions of AG's gray matter (cortical) and WM (subcortical) structures separately in the right and left hemispheres. Accordingly, while AG is associated with functions such as anomia (WM + cortical), phonological (WM), spatial perception (WM), and speech articulation (WM + cortical) in the left hemisphere, anomia (WM + cortical), comprehension (WM + cortical), somatosensory (WM + cortical), spatial perception (WM + cortical) and visual (WM + cortical) functions in the right hemisphere. All these studies in the literature evaluated AG as functional, but our study is the first to classify AG by combining dissection and tractography findings of sAG and IAG in detail.

There is no agreement in the terminology of SLF. The frontoparietal network was first classified as SLF I, II, and III by Petrides and Pandya (1984). There are publications stating that SLF is a single entity (Christiaens et al. 2015; Lerma-Usabiaga et al. 2019), or that questioning the existence of SLF I (Wang et al. 2017), or that SLF II and III are entirely independent entities from SLF I (Komaitis et al. 2019). AF is a group of fibers connecting the frontal and temporal cortices and is independent of the classical SLF components (Martino et al. 2013; Fernández-Miranda et al. 2015; Barbeau et al. 2020). In a recent study (Schurr et al. 2020), SLF II and III boundaries were tried to be separated in tractography using three different datasets. They focused on SLF III and pointed out that the SLF III projects to AG, especially in the right hemisphere. They didn't divide AG into parts; however, the SLF III covers only the sAG on their tractographic demonstrations. In contrast, we did not notice any connections between SLF III and the AG based on our dissections. The classically defined SLF II relationship with sAG and iAG has not been noted so far. Recent publications (Nakajima et al. 2020; Schurr et al. 2020) and our findings reveal that SLF II is associated with sAG. Because of SLF II affects oculomotor function and spatial aspects, Gerstmann syndrome and Spatial hemineglect are observed in its disconnection (Chechlacz et al. 2013;

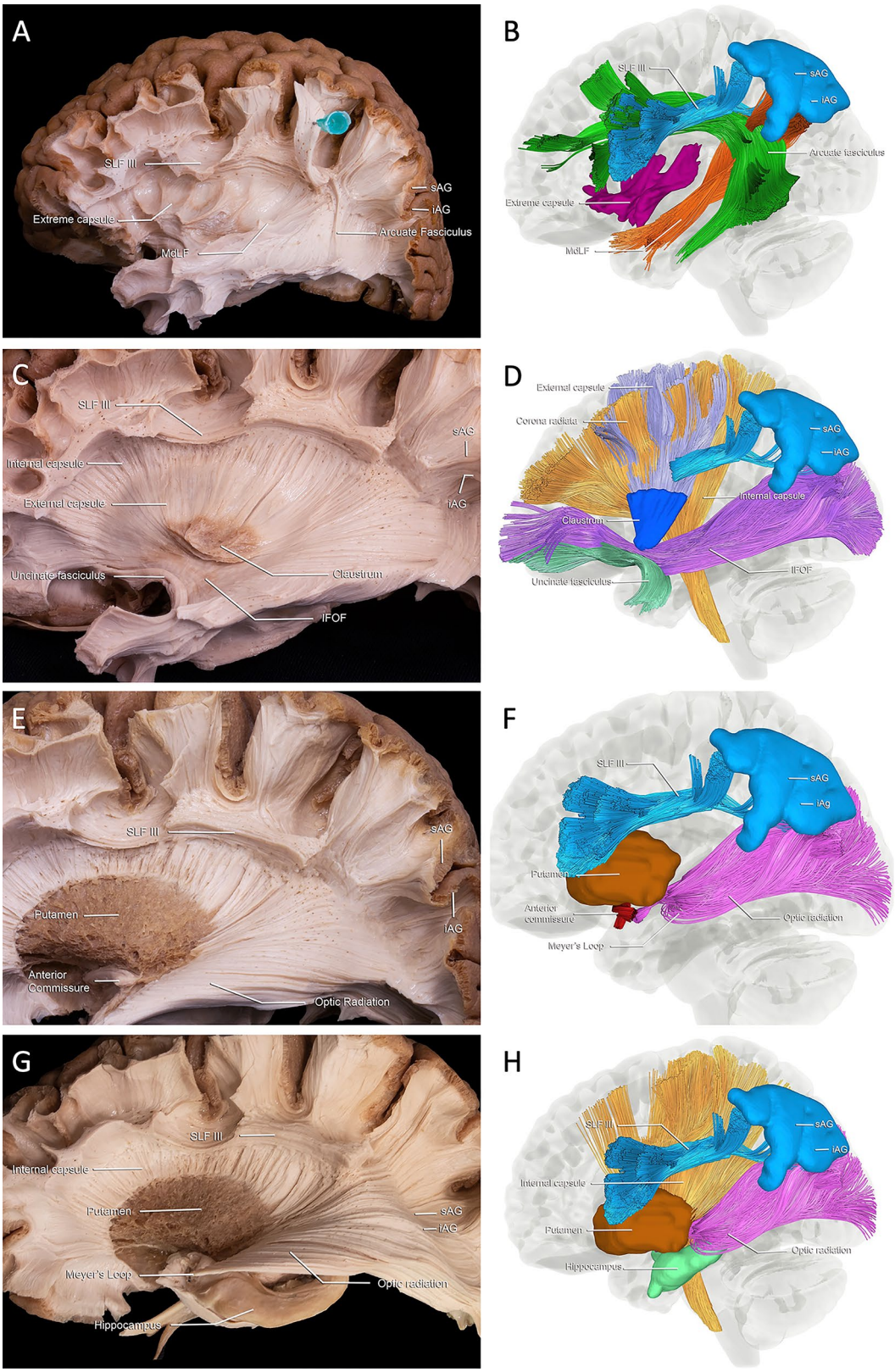

Yagmurlu et al. 2015) (Table 3). The AF connects STG and MTG to MFG and IFG and therefore is in direct contact with both parts of AG.

While fiber dissection studies have shown that the parietal connections of the MdLF are almost completely terminated at the SPL (Maldonado et al. 2013; Wang et al.

◂**Fig. 2** White matter dissection and tractography images in the cadaveric hemisphere without vascular structures. SLF III fibers were preserved throughout the dissection to ensure orientation. **a** The anterior part of the arcuate fasciculus fibers was retracted with the injector to reveal the course of the MdLF fibers. SLF III fibers starting from IFG and then arcuate fasciculus fibers are named at this stage of the dissection. After removing the temporal lobe gray matter and U fibers, MdLF fibers were exposed above STS. When the insula gray matter was removed, extreme capsule was observed. **b** The pathways shown in **a** are presented on the tractography. **c** When the extreme capsule was removed, the external capsule, claustrum, and IFOF fibers were observed. The internal capsule fibers and uncinate fasciculus were revealed when the dissection was deepened. **d** The interrelationships of the fibers shown in **c** are shown in the tractography images. **e** When the external capsule was lifted along the claustrum, the putamen was observed. After removing the IFOF fibers, anterior commissure fibers were detected, and optic radiation was revealed in the deep sagittal stratum posteriorly. **f** In the tractography, the relations of the fibers mentioned in **e** with the putamen and AG are shown. **g**, **h** Internal capsule fibers were not marked in **e**, Meyer's loop of optical radiation, and hippocampus are shown in the cadaver and the tractography image. *sAG* superior angular gyrus; *iAG* inferior angular gyrus; *SLF* superior longitudinal fasciculus; *MdLF* middle longitudinal fasciculus; *IFOF* inferior frontooccipital fasciculus

2013), DTI studies have also shown connections to the IPL (Menjot de Champfleur et al. 2013; Makris et al. 2017). In current studies, MdLF has been divided into many different functional units, but the AG was considered a single unit (Latini et al. 2021; Makris et al. 2017; Kalyvas et al. 2020). A recent study (Latini et al. 2021) divided the MdLF into anterior (deeper brunch) and posterior (superficial branch) parts. Anterior MdLF connects anterior STG and planum polare. Posterior MdLF connects posterior STG, anterior transverse temporal gyrus, planum temporale, and the parieto-occipital region. For the first time in the literature, it has been described that when the AG is divided into two parts, the MdLF fibers progress at the level of the superior AG and form the roof of the iAG. MdLF takes part in processing the spatial features of sounds, but the disconnection syndrome is unknown (Wang et al. 2013; Güngör et al. 2017) (Table 3).

The IFOF originates in parietal and occipital lobes and terminates in the inferior frontal lobe (Motomura et al. 2014). Adjacent to the inferolateral insula, the IFOF courses along with the UF (Kier et al. 2004). Based on its relationship with the central insular sulcus, the IFOF is divided into two parts: anterior and posterior (Güngör et al. 2017). To reach the occipital lobe, the anterior part runs lateral to the inferior of frontal horn, and the posterior part runs lateral to the temporal horn and inferior to the atrium. The anterior and posterior parts run roughly deep into the sAG and iAG. The IFOF takes part in lexical–semantic and visual–spatial processing. The disconnection of IFOF fibers includes semantic paraphasias and nonword reading (Duffau et al. 2005; Rollans et al. 2017) (Table 3).

The OR fibers lie deep to the AC and SS fibers and courses lateral to the temporal horn and inferior two-thirds of the atrium. The OR fibers will be at the iAG level when evaluated according to the cortical surface. The Tp, consisting of splenial callosal fibers surrounding the lateral wall and roof of the atrium, and occipital and temporal horns, is located between the ventricular ependyma and the OR fibers (Yakar et al. 2018). Tp fibers run deep in both parts of the AG. The functions and disconnection

Table 3 The functions of the fibers relevant to AG

Fibers	Function	Disconnection syndrome
SLF II (Chechlacz et al. 2013; Yagmurlu et al. 2015)	Oculomotor and aspects of spatial function	Gerstmann syndrome, spatial hemineglect
AF (Vassal et al. 2013; Chan-Seng et al. 2014; Yagmurlu et al. 2016; Güngör et al. 2017)	Lexical, semantic, and phonological language processing	Transcortical motor aphasia Phonological paraphasia Repetition disorder aphasia
MdLF (Wang et al. 2013; Güngör et al. 2017)	Processing the spatial features of sounds	Unknown
IFOF (Duffau et al. 2005; Rollans et al. 2017)	Lexical-semantic processing Visual-spatial processing	Semantic paraphasias Orthography–phonology translation (nonword reading)
AC (Yagmurlu et al. 2015; Güngör et al. 2017)	Olfactory, auditory, and visual communication	Verbal anosmia
OR (Benjamin et al. 2014; Yagmurlu et al. 2015; Güngör et al. 2017)	Visual	Anterior part: superior homonymous quadrantanopsia Posterior part: homonymous inferior quadrantanopia Central part: macular visual defects
Tp (Pustina et al. 2014; Güngör et al. 2017; Yakar et al. 2018)	Goal-directed actions	Contralateral epileptiform activities Auditory or visual disconnection syndromes

AG angular gyrus, *SLF II* superior longitudinal fasciculus II, *AF* arcuate fasciculus, *MdLF* middle longitudinal fasciculus, *IFOF* inferior frontooccipital fasciculus, *AC* anterior commissure, *OR* optic radiation, *Tp* tapetum

syndromes of all relevant fibers to AG are summarized in Table 3.

As a limitation, we did not compare the tractography and fiber dissection findings in this study. In a study comparing fiber dissection and tractography findings in the temporo-parietal fiber intersection area (Martino et al. 2013), seven tracts were evaluated: posterior portion of the SLF, AF, inferior longitudinal fasciculus (ILF), MdLF, IFOF, OR, and Tp. Accordingly, AF, ILF, IFOF, OR, and Tp were present in all dissections and tractographies. While the posterior portion of the SLF and MdLF were detected in all tractographies, their detection rates in dissections were 75% and 25%, respectively. Since ILF is not adjacent to AG, our study did not include these fibers. Also, we were not able to present all anatomical variants due to the limited number of specimens.

In conclusion, AG was divided into sAG and iAG based on STS in this study. Although it has been shown in previous studies that there are functionally different subunits with AG parcellation, here, for the first time, various functions of the subunits have been revealed with cadaveric dissection and tractography images. Therefore, in surgical interventions for AG, this parcellation of AG will be more efficacious in predicting related complications.

Acknowledgements This research was made possible due to the selfless gift from donor-cadaver patients. We are very grateful for their sacrifice.

Funding The authors declare that no funds, grants, or other support were received during the preparation of this manuscript.

Data availability The datasets generated during and/or analyzed during the current study are available from the corresponding author on reasonable request.

Declarations

Conflict of interest The authors have no relevant financial or non-financial interests to disclose.

Ethical approval This study was performed in line with the principles of the Declaration of Helsinki. Approval was granted by the. Ethics Committee of Pamukkale University (Date: 30.11.2021/No: 21).

References

Barbeau EB, Descoteaux M, Petrides M (2020) Dissociating the white matter tracts connecting the temporo-parietal cortical region with frontal cortex using diffusion tractography. Sci Rep 10(1):8186

Biceroglu H, Karadag A (2019) Neuroanatomical aspects of the temporo-parieto-occipital junction and new surgical strategy to preserve the associated tracts in junctional lesion surgery: fiber separation technique. Turk Neurosurg 29(6):864–874

Binder JR, Desai RH, Graves WW, Conant LL (2009) Where is the semantic system? A critical review and meta-analysis of 120 functional neuroimaging studies. Cereb Cortex 19(12):2767–2796

Benjamin CF, Singh JM, Prabhu SP, Warfield SK (2014) Optimization of tractography of the optic radiations. Hum Brain Mapp 35(2):683–697

Briggs RG, Tanglay O, Dadario NB, Young IM, Fonseka RD, Hormovas J, Dhanaraj V, Lin YH, Kim SJ, Bouvette A, Chakraborty AR, Milligan TM, Abraham CJ, Anderson CD, O'Donoghue DL, Sughrue ME (2021) The unique fiber anatomy of middle temporal gyrus default mode connectivity. Oper Neurosurg (hagerstown) 15 21(1):E8–E14

Burks JD, Boettcher LB, Conner AK, Glenn CA, Bonney PA, Baker CM, Briggs RG, Pittman NA, O'Donoghue DL, Wu DH, Sughrue ME (2017) White matter connections of the inferior parietal lobule: a study of surgical anatomy. Brain Behav 7(4):e00640

Chan-Seng E, Moritz-Gasser S, Duffau H (2014) Awake mapping for low-grade gliomas involving the left sagittal stratum: anatomofunctional and surgical considerations. J Neurosurg 120(5):1069–1077

Chechlacz M, Rotshtein P, Hansen PC, Deb S, Riddoch MJ, Humphreys GW (2013) The central role of the temporo-parietal junction and the superior longitudinal fasciculus in supporting multi-item competition: evidence from lesion-symptom mapping of extinction. Cortex 49:487–506

Christiaens D, Reisert M, Dhollander T, Sunaert S, Suetens P, Maes F (2015) Global tractography of multishell diffusion-weighted imaging data using a multi-tissue model. Neuroimage 123:89–101

Cikla U, Swanson KI, Tumturk A, Keser N, Uluc K, Cohen-Gadol A, Baskaya MK (2016) Microsurgical resection of tumors of the lateral and third ventricles: operative corridors for difficult-to-reach lesions. J Neurooncol 130(2):331–340

Di Carlo DT, Benedetto N, Duffau H, Cagnazzo F, Weiss A, Castagna M, Cosottini M, Perrini P (2019) Microsurgical anatomy of the sagittal stratum. Acta Neurochir (wien) 161(11):2319–2327

Duffau H, Gatignol P, Mandonnet E, Peruzzi P, Tzourio-Mazoyer N, Capelle L (2005) New insights into the anatomo-functional connectivity of the semantic system: a study using cortico-subcortical electrostimulations. Brain 128(4):797–810

Dziedzic TA, Balasa A, Jeżewski MP, Michałowski Ł, Marchel A (2021) White matter dissection with the Klingler technique: a literature review. Brain Struct Funct 226(1):13–47

Egemen E, Celtikci P, Dogruel Y, Yakar F, Sahinoglu D, Farouk M, Adiguzel E, Ugur HC, Coskun E, Güngör A (2021) Microsurgical and tractographic anatomical study of transtemporal-transchoroidal fissure approaches to the ambient cistern. Oper Neurosurg (hagerstown) 20(2):189–197

Fernández-Miranda JC, Wang Y, Pathak S, Stefaneau L, Verstynen T, Yeh FC (2015) Asymmetry, connectivity, and segmentation of the arcuate fascicle in the human brain. Brain Struct Funct 220(3):1665–1680

Güngör A, Baydin S, Middlebrooks EH, Tanriover N, Isler C, Rhoton AL Jr (2017) The white matter tracts of the cerebrum in ventricular surgery and hydrocephalus. J Neurosurg 126(3):945–971

Jitsuishi T, Yamaguchi A (2020) Identification of a distinct association fiber tract "IPS-FG" to connect the intraparietal sulcus areas and fusiform gyrus by white matter dissection and tractography. Sci Rep 10(1):15475

Kadri PAS, de Oliveira JG, Krayenbühl N, Türe U, de Oliveira EPL, Al-Mefty O, Ribas GC (2017) Surgical approaches to the temporal horn: an anatomic analysis of white matter tract interruption. Oper Neurosurg (hagerstown) 13(2):258–270

Kalyvas A, Koutsarnakis C, Komaitis S, Karavasilis E, Christidi F, Skandalakis GP, Liouta E, Papakonstantinou O, Kelekis N, Duffau H, Stranjalis G (2020) Mapping the human middle longitudinal fasciculus through a focused anatomo-imaging study: shifting

the paradigm of its segmentation and connectivity pattern. Brain Struct Funct 225:85–119
Kier EL, Staib LH, Davis LM, Bronen RA (2004) MR imaging of the temporal stem: anatomic dissection tractography of the uncinate fasciculus, inferior occipitofrontal fasciculus, and Meyer's loop of the optic radiation. Am J Neuroradiol 25(5):677–691
Kiriyama I, Miki H, Kikuchi K, Ohue S, Matsuda S, Mochizuki T (2009) Topographic analysis of the inferior parietal lobule in high-resolution 3D MR imaging. AJNR Am J Neuroradiol 30(3):520–524
Komaitis S, Skandalakis GP, Kalyvas AV, Drosos E, Lani E, Emelifeonwu J, Liakos F, Piagkou M, Kalamatianos T, Stranjalis G, Koutsarnakis C (2019) Dorsal component of the superior longitudinal fasciculus revisited: novel insights from a focused fiber dissection study. J Neurosurg 132(4):1265–1278
Latini F, Trevisi G, Fahlström M, Jemstedt M, AlberiusMunkhammar Å, Zetterling M, Hesselager G, Ryttlefors M (2021) New insights into the anatomy, connectivity and clinical implications of the middle longitudinal fasciculus. Front Neuroanat 14:610324
Lerma-Usabiaga G, Mukherjee P, Ren Z, Perry ML, Wandell BA (2019) Replication and generalization in applied neuroimaging. Neuroimage 202:116048
Makris N, Zhu A, Papadimitriou GM, Mouradian P, Ng I, Scaccianoce E, Baselli G, Baglio F, Shenton ME, Rathi Y, Dickerson B, Yeterian E, Kubicki M (2017) Mapping temporo-parietal and temporo-occipital cortico-cortical connections of the human middle longitudinal fascicle in subject-specific, probabilistic, and stereotaxic talairach spaces. Brain Imaging Behav 11(5):1258–1277
Maldonado IL, de Champfleur NM, Velut S, Destrieux C, Zemmoura I, Duffau H (2013) Evidence of a middle longitudinal fasciculus in the human brain from fiber dissection. J Anat 223(1):38–45
Mars RB, Jbabdi S, Sallet J, O'Reilly JX, Croxson PL, Olivier E, Noonan MP, Bergmann C, Mitchell AS, Baxter MG, Behrens TE, Johansen-Berg H, Tomassini V, Miller KL, Rushworth MF (2011) Diffusion-weighted imaging tractography-based parcellation of the human parietal cortex and comparison with human and macaque resting-state functional connectivity. J Neurosci 16 31(11):4087–4100
Martino J, Brogna C, Robles SG, Vergani F, Duffau H (2010) Anatomic dissection of the inferior fronto-occipital fasciculus revisited in the lights of brain stimulation data. Cortex 46(5):691–699
Martino J, da Silva-Freitas R, Caballero H, Marco de Lucas E, García-Porrero JA, Vázquez-Barquero A (2013) Fiber dissection and diffusion tensor imaging tractography study of the temporoparietal fiber intersection area. Neurosurgery 72(1):87–97
Menjot de Champfleur N, Lima Maldonado I, Moritz-Gasser S, Machi P, Le Bars E, Bonafé A, Duffau H (2013) Middle longitudinal fasciculus delineation within language pathways: a diffusion tensor imaging study in human. Eur J Radiol 82(1):151–157. https://doi.org/10.1016/j.ejrad.2012.05.034
Motomura K, Fujii M, Maesawa S, Kuramitsu S, Natsume A, Wakabayashi T (2014) Association of dorsal inferior frontooccipital fasciculus fibers in the deep parietal lobe with both reading and writing processes: a brain mapping study. J Neurosurg 121(1):142–148
Naidich TP, Valavanis AG, Kubik S (1995) Anatomic relationships along the low-middle convexity: part I-normal specimens and magnetic resonance imaging. Neurosurgery 36(3):517–532
Nakajima R, Kinoshita M, Shinohara H, Nakada M (2020) The superior longitudinal fascicle: reconsidering the fronto-parietal neural network based on anatomy and function. Brain Imaging Behav 14(6):2817–2830
Pastor-Escartín F, García-Catalán G, Holanda VM, Muftah Lahirish IA, Quintero RB, Neto MR, Quilis-Quesada V, Ibaoc KB, González Darder JM, de Oliveira E (2019) Microsurgical anatomy of the insular region and operculoinsular association fibers and its neurosurgical application. World Neurosurg 129:407–420
Petrides M, Pandya DN (1984) Projections to the frontal cortex from the posterior parietal region in the rhesus monkey. J Comp Neurol 228(1):105–116
Price AR, Bonner MF, Peelle JE, Grossman M (2015) Converging evidence for the neuroanatomic basis of combinatorial semantics in the angular gyrus. J Neurosci 35(7):3276–3284
Pustina D, Doucet G, Skidmore C, Sperling M, Tracy J (2014) Contralateral interictal spikes are related to tapetum damage in left temporal lobe epilepsy. Epilepsia 55(9):1406–1414
Rademacher J, Galaburda AM, Kennedy DN, Filipek PA, Caviness VS Jr (1992) Human cerebral cortex: localization, parcellation, and morphometry with magnetic resonance imaging. J Cogn Neurosci 4(4):352–374
Ramanan S, Piguet O, Irish M (2018) Rethinking the role of the angular gyrus in remembering the past and imagining the future: the contextual integration model. Neuroscientist 24(4):342–352
Rhoton AL Jr (2007) The cerebrum. Anatomy. Neurosurgery 61(1):37–118 (**discussion 118–119**)
Ribas GC (2010) The cerebral sulci and gyri. Neurosurg Focus 28(2):E2
Ribas EC, Yagmurlu K, de Oliveira E, Ribas GC, Rhoton A (2018) Microsurgical anatomy of the central core of the brain. J Neurosurg 129(3):752–769
Ripollés P, Biel D, Peñaloza C, Kaufmann J, Marco-Pallarés J, Noesselt T, Rodríguez-Fornells A (2017) Strength of temporal white matter pathways predicts semantic learning. J Neurosci 37(46):11101–11113
Rollans C, Cheema K, Georgiou GK, Cummine J (2017) Pathways of the inferior frontal occipital fasciculus in overt speech and reading. Neuroscience 364:93–106
Saalasti S, Alho J, Bar M, Glerean E, Honkela T, Kauppila M, Sams M, Jääskeläinen IP (2019) Inferior parietal lobule and early visual areas support elicitation of individualized meanings during narrative listening. Brain Behav 9(5):e01288
Sarubbo S, De Benedictis A, Merler S, Mandonnet E, Barbareschi M, Dallabona M, Chioffi F, Duffau H (2016) Structural and functional integration between dorsal and ventral language streams as revealed by blunt dissection and direct electrical stimulation. Hum Brain Mapp 37(11):3858–3872
Sarubbo S, Tate M, De Benedictis A, Merler S, Moritz-Gasser S, Herbet G, Duffau H (2020) Mapping critical cortical hubs and white matter pathways by direct electrical stimulation: an original functional atlas of the human brain. Neuroimage 205:116237
Schurr R, Zelman A, Mezer AA (2020) Subdividing the superior longitudinal fasciculus using local quantitative MRI. Neuroimage 208:116439
Seghier ML (2013) The angular gyrus: multiple functions and multiple subdivisions. Neuroscientist 19(1):43–61
Seghier ML, Fagan E, Price CJ (2010) Functional subdivisions in the left angular gyrus where the semantic system meets and diverges from the default network. J Neurosci 30(50):16809–16817
Vassal F, Schneider F, Sontheimer A, Lemaire JJ, Nuti C (2013) Intraoperative visualisation of language fascicles by diffusion tensor imaging-based tractography in glioma surgery. Acta Neurochir 155(3):437–448
Wang J, Fan L, Zhang Y, Liu Y, Jiang D, Zhang Y, Yu C, Jiang T (2012) Tractography-based parcellation of the human left inferior parietal lobule. Neuroimage 63(2):641–652
Wang Y, Fernández-Miranda JC, Verstynen T, Pathak S, Schneider W, Yeh FC (2013) Rethinking the role of the middle longitudinal fascicle in language and auditory pathways. Cereb Cortex 23(10):2347–2356

Wang J, Xie S, Guo X, Becker B, Fox PT, Eickhoff SB, Jiang T (2017) Correspondent functional topography of the human left inferior parietal lobule at rest and under task revealed using resting-state FMRI and coactivation based parcellation. Hum Brain Mapp 38(3):1659–1675

Yagmurlu K, Vlasak AL, Rhoton AL Jr (2015) Three-dimensional topographic fiber tract anatomy of the cerebrum. Neurosurgery 11(Suppl 2):274–305 (**discussion 305**)

Yagmurlu K, Middlebrooks EH, Tanriover N, Rhoton AL Jr (2016) Fiber tracts of the dorsal language stream in the human brain. J Neurosurg 124(5):1396–1405

Yakar F, Eroglu U, Peker E, Armagan E, Comert A, Ugur HC (2018) Structure of corona radiata and tapetum fibers in ventricular surgery. J Clin Neurosci 57:143–148

Yeh FC, Tseng WY (2011) NTU-90: a high angular resolution brain atlas constructed by q-space diffeomorphic reconstruction. Neuroimage 58(1):91–99